

Determination of spin polarization using an unconventional iron superconductor

J. A. Gifford, B. B. Chen, J. Zhang, G. J. Zhao, D. R. Kim, B. C. Li, D. Wu, and T. Y. Chen

Citation: *AIP Advances* **6**, 115023 (2016); doi: 10.1063/1.4968620

View online: <http://dx.doi.org/10.1063/1.4968620>

View Table of Contents: <http://aip.scitation.org/toc/adv/6/11>

Published by the [American Institute of Physics](#)

Articles you may be interested in

[Zero bias anomaly in Andreev reflection spectroscopy](#)

Journal of Applied Physics **120**, 163901 (2016); 10.1063/1.4965983

[Superconducting single X-ray photon detector based on \$W_{0.8}Si_{0.2}\$](#)

AIP Advances **6**, 115104 (2016); 10.1063/1.4967278

[Spin-wave dispersion of nanostructured magnonic crystals with periodic defects](#)

AIP Advances **6**, 115106 (2016); 10.1063/1.4967334

[The physics of photon induced degradation of perovskite solar cells](#)

AIP Advances **6**, 115114 (2016); 10.1063/1.4967817

[Continuous control of spin polarization using a magnetic field](#)

Applied Physics Letters **108**, 212401 (2016); 10.1063/1.4952437

[Analysis on the anisotropic electromechanical properties of lead magnoniobate titanate single crystal for ring type ultrasonic motors](#)

AIP Advances **6**, 115017 (2016); 10.1063/1.4967823

HAVE YOU HEARD?

Employers hiring scientists and
engineers trust

PHYSICS TODAY | JOBS

www.physicstoday.org/jobs



Determination of spin polarization using an unconventional iron superconductor

J. A. Gifford,¹ B. B. Chen,² J. Zhang,¹ G. J. Zhao,¹ D. R. Kim,¹ B. C. Li,¹
 D. Wu,² and T. Y. Chen^{1,a}

¹Department of Physics, Arizona State University, Tempe, AZ 85287, USA

²Department of Physics, National Laboratory of Solid State Microstructures, Nanjing University, China

(Received 14 July 2016; accepted 12 November 2016; published online 21 November 2016)

An unconventional iron superconductor, $\text{SmO}_{0.7}\text{F}_{0.3}\text{FeAs}$, has been utilized to determine the spin polarization and temperature dependence of a highly spin-polarized material, $\text{La}_{0.67}\text{Sr}_{0.33}\text{MnO}_3$, with Andreev reflection spectroscopy. The polarization value obtained is the same as that determined using a conventional superconductor Pb but the temperature dependence of the spin polarization can be measured up to 52 K, a temperature range, which is several times wider than that using a typical conventional superconductor. The result excludes spin-parallel triplet pairing in the iron superconductor. © 2016 Author(s). All article content, except where otherwise noted, is licensed under a Creative Commons Attribution (CC BY) license (<http://creativecommons.org/licenses/by/4.0/>). [<http://dx.doi.org/10.1063/1.4968620>]

In a superconductor (SC), two electrons are bound together with proper spin configuration to form a Cooper pair. In a singlet SC, two electrons must pair with opposite spins whereas in a triplet SC, two electrons can pair with parallel spins. When a current is injected from a normal metal into a SC, the normal current must be converted into a supercurrent. For each injected electron from the normal metal, it must be accompanied by another electron with proper spin to form a Cooper pair to propagate in the SC, consequently reflecting a hole back into the normal metal. This is known as Andreev reflection,¹ which is limited by the availability of electrons with the required spin direction at the Fermi level. The spin alignment of conduction electrons is measured by spin polarization (P), defined as the imbalance of spin-up and spin-down electrons at the Fermi level (E_F) normalized by the total number of electrons, $P = \frac{N_{\uparrow}(E_F) - N_{\downarrow}(E_F)}{N_{\uparrow}(E_F) + N_{\downarrow}(E_F)}$. For an interface between a normal metal with $P = 0$ and a singlet SC, Andreev reflection occurs for each electron with energy less than the superconducting gap (Δ), whereas $P = 1$ for a half-metal, and the conductance is zero within the gap because of the absence of Andreev reflection. By scanning the energy of the injected electrons, Andreev reflection spectroscopy (ARS) or point contact Andreev reflection (PCAR) where the interface is realized by a point contact, can measure the P value of the normal metal^{2–10} and the Δ value of the SC.^{11–13} Within the gap of a spin-parallel triplet pairing SC, however, Andreev reflection can occur even for a half-metallic current. Thus, the P value cannot be measured, distinctively different from that of singlet SC. Triplet SCs are very rare and are experimentally hard to verify.^{14,15} A highly spin-polarized current can thus verify triplet superconductivity via ARS.

High P values can greatly improve spintronics performance and ARS has been extensively utilized to search for highly spin-polarized materials.^{2–10} The P and Δ are determined by analyzing the ARS spectra with a modified Blonder, Tinkham, and Klapwijk (BTK) model¹⁶ with factors such as interfacial scattering (Z), inelastic scattering (Γ), temperature (T), and extra resistance (r_e) included in analysis.^{17–20} In most studies, a conventional SC with transition temperature $T_c < 10$ K and critical field $H_c < 1$ kOe is used. Thus, P is often measured without variation of T and only at zero magnetic field (H). The effect of T on P can be utilized to evaluate the performance of spintronics as well as to reveal important new physics. For example, it is still unknown how P changes across magnetic phase

^aElectronic mail: tingyong.chen@asu.edu

transitions. In addition, the recent discovered topological spin textures^{21–23} often exist in a certain T and H range, and hence a scan of T and H is required to study P in these magnetic structures using ARS. Conventional SCs often have T_c less than 10 K and H_c less than 1 kOe, which are not suitable to explore these features. Unconventional SCs can have much higher T_c and much larger H_c , but they have not been utilized to determine P of magnetic materials, especially highly spin-polarized material or half metals using ARS.

The recently discovered Fe SCs are unconventional with T_c up to 55 K and H_c estimated up to 122 T,²⁴ and their gap structures have been measured by ARS.^{12,13} However, but they have never been utilized to determine the P value of magnetic materials. It has also been predicted that the Fe SCs are spin-triplet.²⁵ A highly spin-polarized material can reveal if there is spin-parallel triplet pairing in the Fe SCs. In this work, we show that P and its temperature dependence of a highly spin-polarized material can be determined using an unconventional Fe SC. The P value of the magnetic material and the Δ value of the Fe SC can be determined simultaneously from 1.5 K to 52 K using a single point contact. The ARS gives rise to the same P value as that obtained using a conventional SC, Pb, and most importantly excludes any spin-parallel triplet pairing in the Fe SC.

Perovskite $\text{La}_{0.67}\text{Sr}_{0.33}\text{MnO}_3$ (LSMO) has been predicted to be a half metal²⁶ and a P value as high as 80% has been measured by ARS.^{8,27} In this work, 100-nm LSMO epitaxial thin film grown by pulse laser deposition²⁸ is used. Its Curie temperature is above 360 K, as shown by the inset of the Fig. 1(a). First, the P value of LSMO was verified by conventional Pb at 1.8 K. Over 20 contacts have been measured and some representative ARS spectra are shown in Fig. 1. The open circles are the experimental data while the solid curves are the best fit to the modified BTK model.¹⁸ As shown in Fig. 1, the ARS spectra display the hallmark double-peak features, with the peak value at about 4 meV. In ARS, the peak value is often an indication of the gap value of the superconductor. However, the Pb wire has $T_c = 7.2$ K and its gap value is 1.34 meV at 1.8 K, much smaller than 4 meV. This is due to the effect of r_E typically observed in samples with large resistivity.¹⁸ In our analysis, Δ is fixed at 1.34 meV, obtained from its $T_c = 7.2$ K, and $T = 1.80$ K is from the experimental value. The value of Γ is fixed as $\Gamma = 0$ because the effect of inelastic scattering is very small using a Pb tip with high purity. In fact, Γ is very close to 0 (< 0.001) even when it is varied in the fitting for all the contacts.

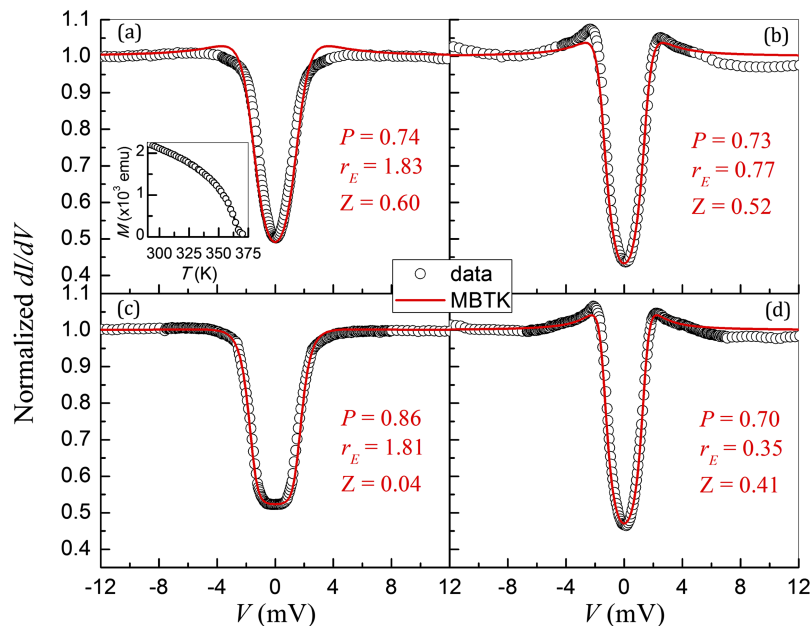


FIG. 1. Representative Andreev spectra (open circles) of contacts between Pb and LSMO film measured at $T = 1.80$ K with the best fits to the modified BTK model (solid curves) where $\Delta = 1.34$ meV, inset of (a) magnetization of LSMO film as a function of temperature.

Only Z , r_E , and P are varied in the analysis, and the obtained P of LSMO is about 80% for small Z , consistent with previous studies.²⁷

There is a small asymmetrical background for all AR spectra in Fig. 1, which has been attributed to mismatch of E_F between Pb and LSMO.²⁷ To understand the background, we measure the T -dependence of ARS spectrum of one contact, as shown in Fig. 2(a), where the spectrum was measured from 1.54 K to over 8 K. For increasing T , the dip of the spectrum increases whereas the two shoulder peaks decrease. Eventually, the spectrum is reduced to a quadratic curve, as shown by the blue curve in Fig. 2(a). The quadratic curve is due to ballistic Joule heating which has been previously studied by some of the authors.²⁹ Clearly, the asymmetry of the ARS spectrum remains above the T_c of Pb, so it has nothing to do with the superconductor, confirming that it is due to the mismatch of E_F between Pb and LSMO.

Above T_c of Pb, the AR spectra at 7.42 K (green) and 7.67 K (blue) are almost the same. One can use the curve above T_c to normalize the AR spectrum at $T < T_c$, and the normalized AR spectra are shown in Fig. 2(b). The spectra are now symmetric and all of them can be well described by the modified BTK model. In our analysis, we first fit the spectrum at $T = 1.54$ K to determine the values of interfacial scattering (Z), inelastic scattering (Γ), extra resistance (r_E), superconducting gap (Δ), and spin polarization (P). The values of Z , Γ and r_E then were fixed for the ARS spectra at $T > 1.54$ K because it is the same contact and there is negligible change in dI/dV outside the gap in the T range, as shown in Fig. 2. In the analysis of each spectrum at different T , only the values of P and Δ were varied. The results are discussed below in Fig. 5.

After verification of the P value in LSMO using conventional Pb, we use the unconventional Fe SC to measure the same LSMO sample. The $\text{SmO}_{0.7}\text{F}_{0.3}\text{FeAs}$ was chosen because it has the

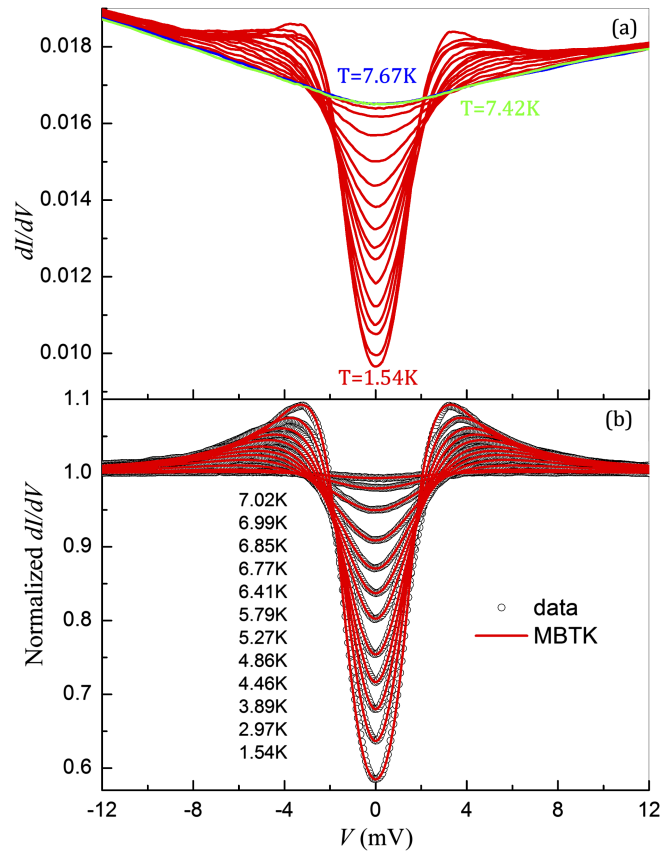


FIG. 2. (a) Andreev spectra of a point contact between Pb and LSMO film from $T = 1.54$ K to 7.67 K, (b) representative Andreev spectra (open circles) with their best fits to the modified BTK model (solid curves) with fitting parameters $\Gamma = 0$, $r_E = 2.19$, $Z = 0.96$, $\Delta(1.54\text{K}) = 1.34$ meV.

highest T_c among the Fe SCs and it has also been theoretically predicted to be spin-triplet.²⁵ The polycrystalline Fe SCs with stoichiometric composition $\text{SmO}_{1-x}\text{F}_x\text{FeAs}$ ($0.1 < x < 0.5$) were synthesized by conventional solid-state reaction and the highest $T_c = 52$ K was obtained with $x = 0.3$, as shown by the inset of Fig. 3(a). The Fe SC was mechanically polished to a tip, then a point contact was established at low T in a vacuum jacket. The ARS spectrum of one Fe SC-LSMO contact from 1.78 K to 53.73 K is shown in Fig. 3(a). Clearly, the conductance is suppressed at $V = 0$ by the high P value in LSMO, but the AR spectrum cannot be analyzed by the modified BTK model due to a large quadratic background and a similar asymmetry as that of Pb/LSMO contacts shown in Fig. 3(a). For the modified BTK model, the conductance must be flat outside the gap so that it can be normalized by a single conductance value for analysis.

A point contact is only a few nanometers in diameter and any thermal expansion could destroy the contact in T variation. In our system, there is a thermally balanced design for approaching the tip, where thermal expansion of various parts including the sample is compensated by parts made from the same materials and with the same length. A point contact has remained stable from 1.5 K up to over 250 K in our system. For a Fe SC-LSMO contact as shown in Fig. 3(a), the conductance spectra are almost the same at $T = 52.50$ K and 53.73 K. We use the data at 52.5 K to normalize all the spectra, and the results are shown in Fig. 3(b). The spectra are now symmetric and flat outside the gap. All spectra can be well described by the modified BTK model. In the analysis, the values of r_E , Z , and Γ were determined by the spectrum at lowest T , then only P and Δ were varied for higher T . The obtained Δ value of the Fe SC is 8.15 meV at 1.78 K, consistent with previous results¹² and its T -dependence, along with the P values, will be discussed below in Fig. 5. At 1.8 K, many contacts

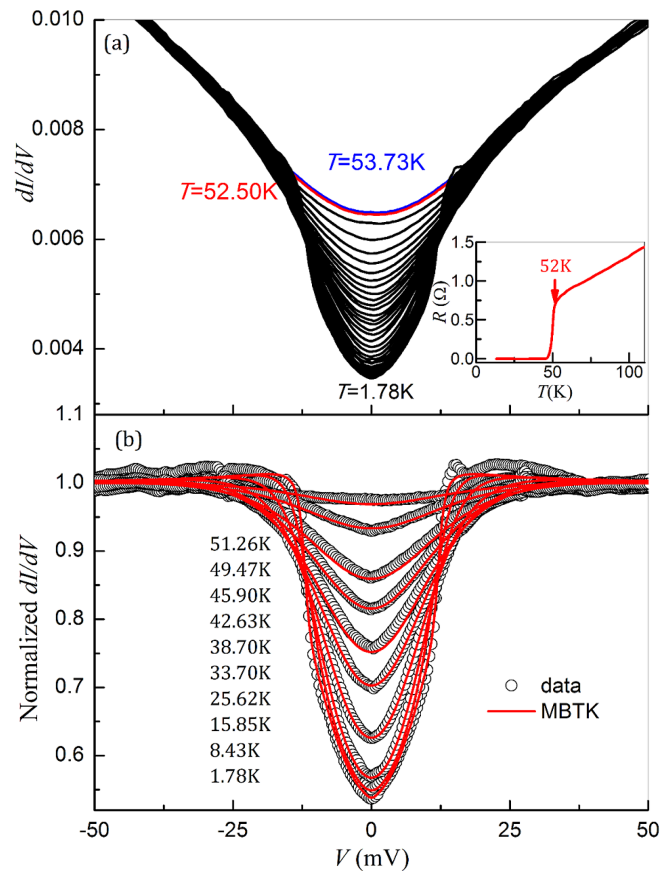


FIG. 3. (a) Andreev spectra of a point contact between Fe SC and LSMO film from $T = 1.78$ K to 53.73 K, (inset) resistance (R) of the Fe SC vs T , (b) representative Andreev spectra (open circles) with their best fits to the modified BTK model (solid curves) with fitting parameters $\Gamma = 0.22$, $r_E = 1.05$, $Z = 0.25$, $\Delta(1.78\text{K}) = 8.15$ meV.

have been measured but they cannot be analyzed until a normalization spectrum of the same contact at $T > T_c$ of the Fe SC is obtained. Using our thermally balanced ARS probe, we have measured several contacts at 1.8 K and over 52 K, and two representative curves are shown in Fig. 4. After normalization, the conductance near $V = 0$ is suppressed by the high P value of LSMO and the spectra can be well described by the modified BTK model. The obtained P and Δ are discussed below.

The values of P and Δ from contacts at various T using both conventional Pb and the unconventional Fe SC are shown in Fig. 5. The P values obtained at low T from Pb tips as a function of Z factor are shown by the open circles in Fig. 5(a). For increasing Z factor, the P value decreases due to spin flip-scattering at the interface, an effect often observed in magnetic materials.⁴⁻¹⁰ Extrapolating to $Z = 0$, the intrinsic P value of LSMO is obtained, which is about $80.9 \pm 3.6\%$. The P values of LSMO obtained from the Fe SC are also shown in Fig. 5(a) as solid squares. They follow the same trend as the results from Pb contacts and give the same intrinsic P value of LSMO. These results show that one can use the Fe SC to measure the P value of a magnetic material, including highly spin-polarized materials.

The T -dependence of the P value for the Pb-LSMO contact in Fig. 2 is shown in Fig. 5(b) as open circles. The P value almost remains constant from 1.5 K to 7.2 K. The P value of the Fe SC/LSMO contact shown in Fig. 3 is shown as solid squares in Fig. 5(b), and again the P value remains constant up to 52 K. This is because the Curie temperature of LSMO is above 360 K, as shown in Fig. 1(a), so that the magnetic properties including the P value do not vary much from 1.5 K to 52 K. In Fig. 5(b), the P value for the Pb/LSMO contact is 0.39 while it is 0.82 for the Fe SC/LSMO contact. The reduced P value is due to the spin-flip scattering at the interface. Indeed, this specific Pb/LSMO contact in Fig. 5(b) has a Z factor of 0.96, much larger than the specific Fe SC/LSMO contact of $Z = 0.25$. This work shows that the P value of a magnetic material can now be measured from 1.5 K to 52 K using ARS, a feat that has never been achieved before. This can be utilized to explore many phase transitions in rare-earth metals³⁰ as well as the recent helical skyrmion crystals^{31,32} which exist below 50 K.

From the T -dependence of the ARS spectra of the Pb and the Fe SC, the Δ values of the two SCs can also be determined simultaneously along with the P values, as shown by the inset of Fig. 5(b). At low T , the Δ value of Pb is 1.42 meV while it is 8.15 meV for the Fe SC. After normalization, the T -dependence of both Pb and the Fe SC are shown in inset of Fig. 5(b), where

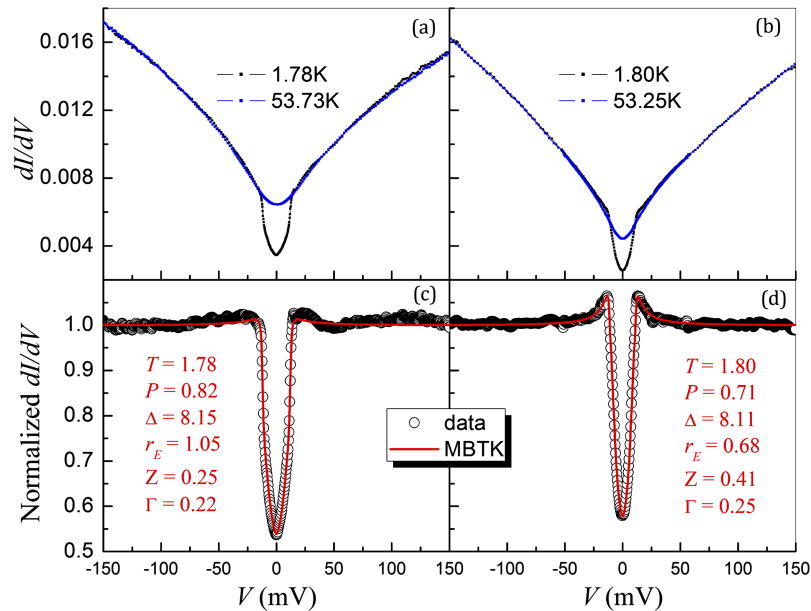


FIG. 4. Representative Andreev spectra of contacts between Fe SC and LSMO film: (a, b) Andreev spectra at low T and normalization spectra $T > 52$ K, (c, d) Normalized Andreev spectra and their best fits to the modified BTK model.

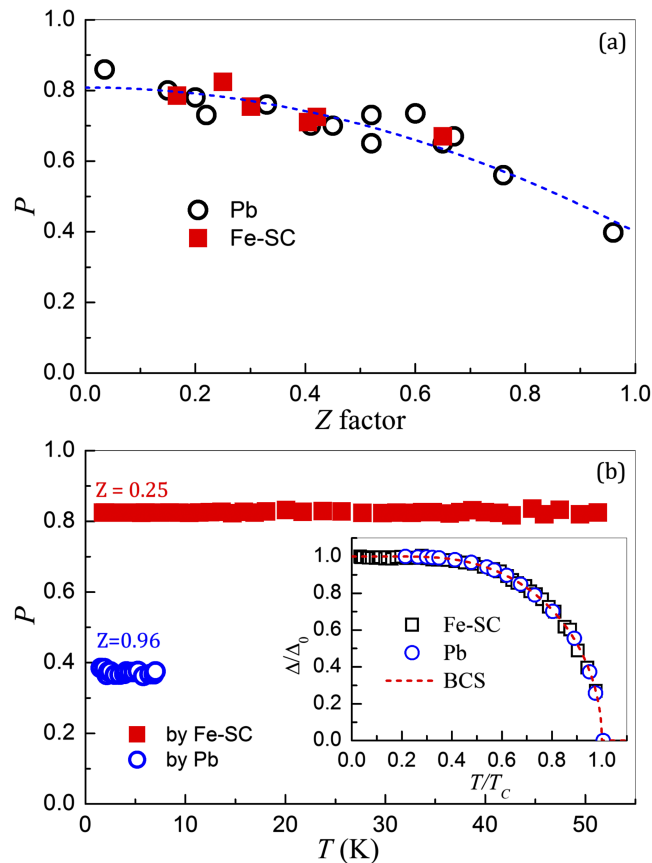


FIG. 5. (a) Spin polarization of LSMO film obtained from Pb (open circles) and Fe SC (solid squares) contacts as function of Z factor, (b) Spin polarization from Pb-LSMO contact (open circle) and Fe SC-LSMO contact (solid square) as function of temperature, and (inset) normalized gap values of Pb and Fe SC as a function of T/T_c where dashed curve is from BCS theory to guide one's eyes.

the dashed curve is from the BCS theory. One can see that the T -dependence of the Fe SC is the same as that of Pb, consistent with previous reports.¹² Furthermore, as discussed above, it has been proposed that the Fe SC could be spin-triplet.²⁵ For a spin-parallel triplet SC, the two electrons in a Cooper pair have the same spin orientation. The Andreev reflection of a half metal should then be the same as that of a nonmagnetic metal, such as gold. This is because two electrons from the half metallic current can form a Cooper pair and thus Andreev reflection occurs to show the double conductance, instead of zero conductance for the singlet case. If there is any spin-parallel triplet pairing in the Fe SC, there will be no suppression of the conductance like those shown in Fig. 3 and 4. The exact the same P value obtained from both the conventional Pb and the unconventional Fe SC using the same LSMO material demonstrates that there is no spin-parallel triplet pairing in the Fe SC.

In summary, we have shown that an unconventional Fe SC can be utilized to determine spin polarization of highly spin-polarized materials in ARS with proper normalization and it gives the same value as that using a conventional SC. The Fe SC can measure spin polarization in a much wider temperature range up to 52 K, which is over five times larger than for a typical conventional SC. Most importantly, a highly spin-polarized current reveals that there is no spin-triplet component in the Fe SC, $\text{SmO}_{0.7}\text{F}_{0.3}\text{FeAs}$.

ACKNOWLEDGMENTS

This work was supported as part of SHINES, an EFRC center funded by the U. S. Department of Energy, Office of Science, Basic Energy Science, under award SC0012670.

- ¹ A. F. Andreev, Zh. Eksp. Teor. Fiz. **46**, 1823 (1964); [Sov. Phys. JETP **19**, 1228 (1964)].
- ² S. K. Upadhyay, A. Palanisami, R. N. Louie, and R. A. Buhrman, *Phys. Rev. Lett.* **81**, 3247 (1998).
- ³ R. J. Soulen, Jr., J. M. Byers, M. S. Osofsky, B. Nadgorny, T. Ambrose, S. F. Cheng, P. R. Broussard, C. T. Tanaka, J. Nowak, J. S. Moodera, A. Barry, and J. M. D. Coey, *Science* **282**, 85 (1998).
- ⁴ G. J. Strijkers, Y. Ji, F. Y. Yang, C. L. Chien, and J. M. Byers, *Phys. Rev. B* **63**, 104510 (2001).
- ⁵ Y. Ji, G. J. Strijkers, F. Y. Yang, C. L. Chien, J. M. Byers, A. Anguelouch, G. Xiao, and A. Gupta, *Phys. Rev. Lett.* **86**, 5585 (2001).
- ⁶ J. S. Parker, S. M. Watts, P. G. Ivanov, and P. Xiong, *Phys. Rev. Lett.* **88**, 196601 (2002).
- ⁷ L. Wang, K. Umemoto, R. M. Wentzcovitch, T. Y. Chen, C. L. Chien, J. G. Checkelsky, J. C. Eckert, E. D. Dahlberg, and C. Leighton, *Phys. Rev. Lett.* **94**, 056602 (2005).
- ⁸ B. Nadgorny, I. I. Mazin, M. Osofsky, R. J. Soulen, Jr., P. Broussard, R. M. Stroud, D. J. Singh, V. G. Harris, A. Arsenov, and Y. Mukovskii, *Phys. Rev. B* **63**, 184433 (2001).
- ⁹ T. Y. Chen, C. L. Chien, and C. Petrovic, *Appl. Phys. Lett.* **91**, 142505 (2007).
- ¹⁰ J. A. Gifford, C. N. Snider, J. Martinez, and T. Y. Chen, *J. Appl. Phys.* **113**, 17B105 (2013).
- ¹¹ G. Blonder and M. Tinkham, *Phys. Rev. B* **27**, 112 (1983).
- ¹² T. Y. Chen, Z. Tesanovic, R. H. Liu, X. H. Chen, and C. L. Chien, *Nature* **453**, 1224 (2008).
- ¹³ T. Y. Chen, S. X. Huang, Z. Tesanovic, R. H. Liu, X. H. Chen, and C. L. Chien, *Physica C* **469**, 521 (2009).
- ¹⁴ Y. Maeno, S. Kittaka, T. Nomura, S. Yonezawa, and K. Ishida, *J. Phys. Soc. Jpn.* **81**, 011009 (2012).
- ¹⁵ Y. Liu and Z.-Q. Mao, *Physica C* **514**, 339 (2015).
- ¹⁶ G. E. Blonder, M. Tinkham, and T. M. Klapwijk, *Phys. Rev. B* **25**, 4515 (1982).
- ¹⁷ T. Y. Chen, Z. Tesanovic, and C. L. Chien, *Phys. Rev. Lett.* **109**, 146602 (2012).
- ¹⁸ T. Y. Chen, S. X. Huang, and C. L. Chien, *Phys. Rev. B* **81**, 214444 (2010).
- ¹⁹ P. Chalsani, S. K. Upadhyay, O. Ozatay, and R. A. Buhrman, *Phys. Rev. B* **75**, 094417 (2007).
- ²⁰ G. T. Woods, R. J. Soulen, Jr., I. I. Mazin, B. Nadgorny, M. S. Osofsky, J. Sanders, H. Srikanth, W. F. Egelhoff, and R. Datla, *Phys. Rev. B* **70**, 054416 (2004).
- ²¹ U. K. Rößler, A. N. Bogdanov, and C. Pfleiderer, *Nature* **442**, 797 (2006).
- ²² S. Mühlbauer, B. Binz, F. Jonietz, C. Pfleiderer, A. Rosch, A. Neubauer, R. Georgii, and P. Böni, *Science* **323**, 915 (2009).
- ²³ X. Z. Yu, Y. Onose, N. Kanazawa, J. H. Park, J. H. Han, Y. Matsui, N. Nagaosa, and Y. Tokura, *Nature* **465**, 901 (2010).
- ²⁴ J. Prakash, S. J. Singh, S. L. Samal, S. Patnaik, and A. K. Ganguli, *EPL* **84**, 57003 (2008).
- ²⁵ P. A. Lee and X.-G. Wen, *Phys. Rev. B* **78**, 144517 (2008).
- ²⁶ W. E. Pickett and D. J. Singh, *J. Magn. Magn. Mater.* **172**, 237 (1997).
- ²⁷ Y. Ji, C. L. Chien, Y. Tomioka, and Y. Tokura, *Phys. Rev. B* **66**, 012410 (2002).
- ²⁸ B. B. Chen, Y. Zhou, S. Wang, Y. J. Shi, H. F. Ding, and D. Wu, *Appl. Phys. Lett.* **103**, 072402 (2013).
- ²⁹ T. Y. Chen, C. L. Chien, M. Manno, L. Wang, and C. Leighton, *Phys. Rev. B Rapid Communication* **81**, 020301 (2010).
- ³⁰ S. Chikazumi, *Physics of Ferromagnetism*, 2nd edition, ISBN 0-19-851776-9, (2005).
- ³¹ S. Mühlbauer, B. Binz, F. Jonietz, C. Pfleiderer, A. Rosch, A. Neubauer, R. Georgii, and P. Böni, *Science* **323**, 915 (2009).
- ³² X. Z. Yu, Y. Onose, N. Kanazawa, J. H. Park, J. H. Han, Y. Matsui, N. Nagaosa, and Y. Tokura, *Nature* **465**, 901–904 (2010).